Infrared Radiation Parameterizations for the Minor CO_2 Bands and for Several CFC Bands in the Window Region

DAVID P. KRATZ

Lockheed Engineering and Sciences Company, Hampton, Virginia

MING-DAH CHOU

Laboratory for Atmospheres, NASA/Goddard Space Flight Center, Greenbelt, Maryland

MICHAEL M.-H. YAN

Science Systems & Application, Inc., Lanham, Maryland

(Manuscript received 9 October 1992, in final form 8 January 1993)

ABSTRACT

Fast and accurate parameterizations have been developed for the transmission functions of the CO_2 9.4- and 10.4-μm bands, as well as the CFC-11, CFC-12, and CFC-22 bands located in the 8–12-μm region. The parameterizations are based on line-by-line calculations of transmission functions for the CO_2 bands and on high spectral resolution laboratory measurements of the absorption coefficients for the CFC bands. Also developed are the parameterizations for the H_2O transmission functions for the corresponding spectral bands. Compared to the high-resolution calculations, fluxes at the tropopause computed with the parameterizations are accurate to within 10% when overlapping of gas absorptions within a band is taken into account. For individual gas absorption, the accuracy is of order 0%–2%.

The climatic effects of these trace gases have been studied using a zonally averaged multilayer energy balance model, which includes seasonal cycles and a simplified deep ocean. With the trace gas abundances taken to follow the Intergovernmental Panel on Climate Change Low Emissions "B" scenario, the transient response of the surface temperature is simulated for the period 1900–2060. The minor CO_2 and CFC bands contribute about 20%–25% of the total warming at the surface, which is comparable to the contribution from the CH_4 and N_2O bands. Collectively, these minor absorption bands account for 40%–45% of the total surface temperature increases. Thus, the climate warming due to absorption in these bands is comparable to that in the 15-μm CO_2 band.

1. Introduction

As concern grows over the potential radiative effects of the various infrared active trace gases currently being dispersed into the atmosphere by anthropogenic activities, it becomes increasingly evident that, to be reliable, climate models must properly take into account the radiative effects of these trace gases. The inclusion of additional absorption bands in a radiative transfer procedure, however, results in an increased demand upon available computer time. Even without considering the radiative effects of the minor trace gases (gases other than CO_2, H_2O, and O_3), calculations involving the radiative terms in general circulation models (GCMs) can easily consume 30% or more of the total computing time. Thus, taking into account the radiatively important trace gases can lead to substantial computing time requirements. As an alternative, Wang et al. (1991a) explored the possibility of employing an effective CO_2 concentration to simulate the combined radiative effects of CO_2 and the other trace gases. They discovered, however, that it is inappropriate to employ an effective CO_2 abundance to simulate the combined radiative effects of CO_2 and the other trace gases, which in their case included CH_4, N_2O, CFC-11, and CFC-12. Wang et al. (1991a) based their conclusion on model results that indicated that the radiative forcing behavior of CO_2 was significantly different from the radiative forcing behaviors of the other trace gases. Thus, efficient yet accurate parameterizations are required for each of the trace gases to be investigated.

Chou et al. (1991) have developed fast and accurate parameterizations for the absorptances due to the thermal infrared bands of H_2O, the 15-μm band of CO_2, the 9.6-μm band of O_3, the 7.7-μm band of CH_4, and several infrared bands of N_2O. While the comprehensive study of Chou et al. (1991) considered the most prominent infrared spectral features due to gaseous ab-

Corresponding author address: Dr. David P. Kratz, Lockheed Engineering and Sciences Co., 144 Research Drive, Hampton, VA 23666.

sorption in the earth's atmosphere, there are a number of other radiatively active trace gases that have been identified (e.g., Ramanathan et al. 1985) as having the potential to alter the climate. We shall focus our attention on some of these other absorption bands.

In this study we develop temperature- and pressure-dependent broadband parameterizations for the 9.4- and 10.4-μm bands of CO_2. We also develop temperature-dependent broadband parameterizations for the infrared spectra of CFC-11, CFC-12, and CFC-22. The spectral ranges of the absorption bands under consideration are presented in Table 1. In order to account for the spectral overlap of the trace gas absorption features with those of H_2O, parameterizations for H_2O are constructed for the appropriate spectral intervals. The absorption parameterizations are based on line-by-line calculations for H_2O and the minor CO_2 bands, and on laboratory measurements for the CFC bands. Incorporating the new parameterizations into the multilayer energy balance model (MLEBM) of Peng et al. (1987) allows for an investigation of both the equilibrium and time-dependent climatic responses to changes in the abundances of the trace gases under consideration.

2. The 9.4- and 10.4-μm CO_2 bands

The relatively weak 9.4- and 10.4-μm bands of CO_2 are nonnegligible contributors to the radiative forcing attributed to the enhanced abundances of CO_2 (Kratz et al. 1991). For instance, for a doubling of the present abundance of CO_2, these minor CO_2 bands will not only contribute about 10% of the infrared radiative forcing at the tropopause, but will also, as compared to the case where only the 15-μm band is considered, enhance by nearly a factor of 3 the resultant cooling in the first few kilometers of the troposphere (Kratz et al. 1991). Moreover, Owen et al. (1979) have shown that for suspected CO_2 abundances present in the earth's early atmosphere, the 9.4- and 10.4-μm bands of CO_2 would effectively close the infrared atmospheric window. Kiehl and Dickinson (1987) further demonstrated that these minor CO_2 bands are critical in maintaining paleoclimatic temperatures above 273 K, and thus are critical in resolving the issue of the faint early sun paradox (Sagan and Mullen 1972). It is therefore necessary to accurately determine the radiative effects of these minor CO_2 bands in models that examine climatic effects of enhancing the abundances of infrared active molecules.

TABLE 1. Spectral ranges of the trace gases under consideration. The quantity, ω_0, is the band center wavenumber.

Band number	Band	ω_0 (cm^{-1})	Wavenumber range (cm^{-1})
1	CO_2 (9.4 μm)	1064	981–1114
2	CO_2 (10.4 μm)	961	863–1007
3	CFC-11 (9.2 μm)	1085	1030–1130
4	CFC-11 (11.8 μm)	846	820–870
5	CFC-12 (8.6/9.1 μm)	1131	1030–1200
6	CFC-12 (10.8 μm)	923	830–950
7	CFC-22 (9.0 μm)	1116	1070–1190
8	CFC-22 (12.4 μm)	809	760–860

Currently, the most accurate approach for calculating molecular line absorption is the line-by-line procedure. For the 9.4- and 10.4-μm bands of CO_2, our line-by-line procedure utilizes the 1986 version of the Air Force Geophysics Laboratory (AFGL) absorption line parameters (Rothman et al. 1987). As noted in Table 1, the 9.4-μm band is taken to cover the wavenumber range from 981 to 1114 cm^{-1}, while the 10.4-μm band is taken to cover the wavenumber range from 863 to 1007 cm^{-1}. As suggested by Kratz et al. (1991), the line shape factors are taken to follow the Voigt function with a wavenumber cutoff of 5 cm^{-1}; that is, the spectral absorption coefficient includes the effects of all the rotational lines within a 10-cm^{-1} range centered at the wavenumber of the absorption coefficient. The interval size for the wavenumber integration is taken to be 0.005 cm^{-1}. This wavenumber resolution, which is approximately equal to the line halfwidth at 70 mb, is able to resolve individual lines in the troposphere. Moreover, Kratz et al. (1991) have demonstrated that finer spectral resolutions yield virtually no change to the flux calculations. Further details of the line-by-line calculations are discussed in Kratz et al. (1991).

While the line-by-line procedure can be used to directly compute the radiative effects of infrared active molecules, it is often desirable to create absorption parameterizations that are based upon the line-by-line procedure. Parameterizing the absorption due to the 9.4- and 10.4-μm bands of CO_2, however, has proved to be somewhat complex owing to the fact that these upper-state bands are quite temperature sensitive. Employing our line-by-line procedure to calculate band absorptances for the 9.4- and 10.4-μm bands of CO_2, we observe that, for conditions appropriate to the present climatic state (e.g., a CO_2 column abundance of $\sim$0.5 gm cm^{-2} and a pressure of 1 atmosphere), the band absorptances for both the 9.4- and 10.4-μm bands of CO_2 increase by nearly an order of magnitude as the temperature is increased from 210 to 290 K. Any parameterization that is considered must be able to handle this extreme temperature sensitivity if accurate absorptances are to be obtained.

The line-by-line procedure was utilized to compute reference band absorptances for 21 CO_2 abundances (ranging from 10^{-4} to 10 gm cm^{-2}), 5 pressures (0.10, 0.25, 0.50, 0.75, and 1.0 atm), and 3 temperatures (210, 250, and 290 K). An eight-point Gaussian quadrature was incorporated into the line-by-line procedure to calculate the diffuse absorptances. Two previous studies, Kiehl and Dickinson (1987), and Kratz et al. (1991), employed the broadband procedure described by Kiehl and Ramanathan (1983) to fit the absorption

curve due to the minor CO_2 bands. While the results of these broadband parameterizations are satisfactory, Chou and Peng (1983) presented a viable alternative model that is somewhat less complex. They found for the 15-μm band of CO_2 that a function similar to that used by Howard et al. (1956),

$$\tau = \frac{aw}{(1 + bw^c)}, \quad (1)$$

accurately reproduced the diffuse absorptances, $A_{diff} = 1 - \exp(-\tau)$, as calculated by the line-by-line procedure. The quantity τ is the diffuse optical depth, w is the CO_2 abundance, and a, b, and c are regression coefficients. Parameterizations employing Eq. (1) or a closely related expression are utilized by the MLEBM developed at the Goddard Space Flight Center (Peng et al. 1987) for a variety of infrared absorption bands. Before proceeding, it must be noted that in computing the 15-μm band CO_2 transmission functions, Chou and Peng (1983) employed a one-parameter scaling for the CO_2 abundance to account for variations in pressure and temperature, and thus their coefficients a, b, and c are independent of pressure and temperature. Unlike the fairly strong absorption bands with moderate temperature dependencies considered by Chou and Peng (1983), the 9.4- and 10.4-μm bands of CO_2 are fairly weak bands with strong temperature dependencies, and therefore, a more flexible two-parameter scaling approximation is required.

Our investigation has found that for the 9.4- and 10.4-μm bands of CO_2, parameterizations in the form of Eq. (1), in which the coefficients a, b, and c depend upon temperature, can yield absorptances within 1% of the results of the line-by-line calculations for the entire range of temperatures and CO_2 abundances at a specific pressure. Since a range of pressures is encountered in the atmosphere, however, we modified Eq. (1) to explicitly include the pressure dependence of the absorption. While several procedures were considered, the functional form

$$\tau = \frac{aw}{(1 + bw^c p^{-y})} \quad (2)$$

maintained a high degree of accuracy while avoiding unnecessary complexity. The pressure, p, in Eq. (2) has the units of atm, and the coefficient y is given by:

$$y = d + \frac{e}{1 + w}, \quad (3)$$

where d and e are regression coefficients. It should be noted that Eq. (2) satisfies the linear limit, and can be made to satisfy the strong nonoverlapping line limit if the coefficients c and y are taken to be ½. Thus, the form of Eq. (3) allows Eq. (2) to follow the theoretical curve of growth while maintaining sufficient flexibility to handle departures from theory. For the present case, we find that the optical depth, τ, is only weakly dependent upon the values of the coefficients, d and e, so long as their sum remains constant. We therefore conclude that the values of these coefficients are merely fine-tuning adjustments for the parameterization. Indeed, if a value of ½ is taken for the coefficients d and e, only a modest discrepancy ($\lesssim$5%) is introduced into the calculated value of τ.

The regression coefficients for our parameterization of the 9.4- and 10.4-μm bands of CO_2 are presented in Table 2. The temperature dependencies of the regression coefficients are given by:

$$a(t) = a(290) + a'(t - 290) + a''(t - 290)^2, \quad (4)$$

$$b(t) = b(290) + b'(t - 290) + b''(t - 290)^2, \quad (5)$$

$$c(t) = c(290) + c'(t - 290), \quad (6)$$

where t is the temperature in kelvin. As noted previously, the absorptances due to the 9.4- and 10.4-μm bands of CO_2 are quite temperature sensitive, and therefore the complexity of Eqs. (4)–(6) was necessary to obtain accurate fits over the range of temperatures under consideration. The reference temperature was chosen to be 290 K since the contribution of these absorption bands to the opacity of the atmosphere is principally found within the first few kilometers from the surface.

While the present parameterizations were fit to a range of CO_2 abundances ranging from 10^{-4} to 10 gm cm^{-2}, comparisons with reference line-by-line calculations revealed that the present parameterizations were able to yield absorptances within 5% for CO_2 abundances as high as 10^3 gm cm^{-2}. Nevertheless, attempts to specifically include this enlarged range of CO_2 abundances resulted in unacceptable degradations to the fit for current CO_2 abundances. Since our study is principally concerned with conditions near those currently present, the smaller range was chosen.

The parameterization presented in Eq. (2) yields very good results when the calculation involves a homogeneous layer with constant temperature and pressure; however, for an inhomogeneous medium such as the earth's atmosphere, the parameterization requires

TABLE 2. Parameters for coupling CO_2 9.4- and 10.4-μm band absorptances. The units for the corresponding abundances, ω, are gm cm^{-2}.

Band	α (290)	a'	a''	b (290)	b'	b''	c (290)	c'	d	e
CO_2 (9.4 μm)	0.18822	3.864×10^{-3}	2.15×10^{-5}	0.6340	9.34×10^{-3}	3.64×10^{-5}	0.730	0.0	0.42	0.70
CO_2 (10.4 μm)	0.11878	2.5733×10^{-3}	1.497×10^{-5}	0.4914	7.88×10^{-3}	3.34×10^{-5}	0.690	-7.5×10^{-4}	0.50	0.60

the inhomogeneous path to be scaled to an equivalent homogeneous path. As noted previously, while the CO_2 absorption bands in the 9.4- and 10.4-μm regions are relatively weak, their temperature dependencies are very strong. Thus, to account for an inhomogeneous atmosphere, a two-parameter scaling approximation is required to account for the effects of temperature and pressure variations. Chou et al. (1991) noted that the effective pressure and temperature are usually computed by weighting them by the absorber amount w along the path and thus can be given by:

$$p_{eff} = \int pdw \left(\int dw \right)^{-1}, \tag{7}$$

$$t_{eff} = \int tdw \left(\int dw \right)^{-1}. \tag{8}$$

It has been established that the contribution to the cooling rate is primarily from adjacent layers, especially within optically thick bands (see, e.g., Wu 1980; Chou and Kouvaris 1991). Since the temperature and pressure variations among nearby layers are usually small, the simple scaling approximation of Eqs. (7) and (8) generally yields accurate cooling rate calculations. Only for distant layers, where the contribution to the flux and cooling rate calculations is typically small, does this scaling approximation normally prove to be inappropriate. Our present case, however, involves highly temperature-sensitive absorptances which, for present CO_2 abundances, are fairly near the optically thin region. This particular scenario is especially taxing on a scaling approximation. Indeed, for the 9.4- and 10.4-μm bands of CO_2, the use of the temperature scaling in Eq. (8) introduces sufficient error (e.g., the errors in the top of the atmosphere fluxes were in excess of 10% for CO_2 mixing ratios of 300 and 600 ppmv) to warrant an alternative formulation.

Since the radiative effects of the temperature-sensitive 9.4- and 10.4-μm bands of CO_2 are greatest within the first few kilometers of the surface, it is anticipated that a scaling approximation that gives even greater weight to the lower portion of the atmosphere than that provided by Eq. (8) might yield improved results. A reasonable modification to Eq. (8) is to weight the temperature with a pressure-dependent function. We found that by employing the scaling

$$t_{eff} = \int tp^{1/2}dw \left(\int p^{1/2}dw \right)^{-1} \tag{9}$$

we could obtain fairly good agreement with the line-by-line results.

In order to facilitate a comparison of the present broadband parameterization to the line-by-line calculations, we have calculated the reductions in the net flux change due to the absorption/emission by the 9.4- and 10.4-μm bands of CO_2. To be compatible with the intercomparison of radiation codes used in climate models (ICRCCM) (Ellingson et al. 1991), we employed the updated version of the midlatitude summer atmosphere of McClatchey et al. (1972) as reported by Ellingson et al. (1991). The net flux reductions at the top of the atmosphere (50 km) and the tropopause (13 km), and the net flux enhancement at the surface are presented in Table 3 for a CO_2 mixing ratio of 300 ppmv, a value consistent with ICRCCM (Ellingson et al. 1991), two times this abundance, and a hundred times this abundance. Note that CO_2 is the only absorber considered for these calculations. Overlapping absorptances by other gases are neglected. Table 3 includes not only a comparison between our line-by-line procedure and our broadband parameterization but also the Goody random-band model (with a spectral resolution of 5 cm^{-1}) employed by Kratz et al. (1991). As can be observed, the present broadband parameterization is comparable in accuracy to the Goody random-band model. Indeed, for large CO_2 abundances, our new parameterization reproduces the results of the line-by-line procedure more accurately than the random-band model. In general, the accuracy of the present parameterization is comparable to the broadband model presented by Kratz et al. (1991) except for very large CO_2 abundances ($\sim$100–1000 times the present abundance) where the present parameterization retains far better accuracy than the Kratz et al. (1991) parameterization. This improved accuracy at high CO_2 abundances is one of the advantages of the present parameterization. Nevertheless, a close examination of Table

TABLE 3. Model calculations of the reduction in the net upward flux (W m^{-2}) at the top of the atmosphere and at the tropopause, and the increase in the downward flux at the surface due to CO_2 absorption in the 9.4- and 10.4-μm bands for CO_2 mixing ratios of 300 ppmv, two times this abundance, and one hundred times this abundance. Overlapping with water vapor absorption is not considered.

Band	Case	Top	Tropopause	Surface
CO_2 (9.4 μm)	1	0.355	0.334	0.881
[300 ppmv]	2	0.358	0.334	0.854
	3	0.356	0.341	0.823
CO_2 (9.4 μm)	1	0.617	0.589	1.531
[600 ppmv]	2	0.623	0.588	1.474
	3	0.621	0.601	1.437
CO_2 (9.4 μm)	1	5.940	6.000	12.870
[30 000 ppmv]	2	5.554	5.623	11.454
	3	5.881	6.199	11.769
CO_2 (10.4 μm)	1	0.278	0.263	0.790
[300 ppmv]	2	0.275	0.259	0.751
	3	0.280	0.269	0.729
CO_2 (10.4 μm)	1	0.498	0.476	1.409
[600 ppmv]	2	0.489	0.465	1.323
	3	0.502	0.487	1.305
CO_2 (10.4 μm)	1	5.790	5.863	14.758
[30 000 ppmv]	2	5.358	5.426	12.870
	3	5.632	6.070	13.396

Case 1 = line-by-line calculation
Case 2 = Goody random-band model
Case 3 = present parameterization

3 will reveal that discrepancies remain between the present parameterization and the reference line-by-line calculations. The source of this difference lies almost entirely in the inability of the scaling approximation to fully cope with such highly temperature-sensitive absorptances as found with these minor CO_2 bands.

3. CFC-11, CFC-12, and CFC-22

Ramanathan (1975) was the first to discuss the potential radiative impact of the release into the atmosphere of order 1 ppbv of CFC-11 and CFC-12. Since the appearance of Ramanathan's report, numerous investigations, for example, Wang et al. (1976), Lacis et al. (1981), Wang and Molnar (1985), Ramanathan et al. (1985), Dickinson and Circerone (1986), Hansen et al. (1988), Hansen et al. (1989), and Wang et al. (1991b) have considered the radiative effects of the chlorofluorocarbons (CFCs). As noted by Kratz and Varanasi (1992), with few exceptions (e.g., Ramanathan et al. 1985; Wang et al. 1991b) a common practice has been to assume that the spectral absorption by the CFCs is adequately parameterized by a broadband formulation based upon the optically thin approximation. In addition, it has been a common procedure to ignore the temperature dependence of the CFC absorption features. Kratz and Varanasi (1992) employed laboratory-measured absorption coefficients of Varanasi (1992) to investigate these and other issues involving the absorption due to CFC-11 and CFC-12. Their investigation indicated that, by ignoring the temperature dependence of the CFC bands and also neglecting the departures of the CFC absorptance from the optically thin approximation, only modest overestimations were introduced for the estimations of the absorption due to projected abundances of CFC-11 and CFC-12. While these results are very encouraging, Kratz and Varanasi (1992) further noted that the errors introduced by the often-used simplifications always tend toward overestimating the radiative effect of the CFCs, and thus when considered as a whole may no longer yield negligible discrepancies. We will therefore refrain from incorporating these limitations into our parameterizations for CFC-11, CFC-12, and CFC-22.

For conditions encountered in the earth's troposphere and stratosphere the spectral features due to CFC-11, CFC-12, and CFC-22 are characterized by line spacings that are significantly smaller than the line halfwidths. The rotational fine structure of the bands are therefore smeared out and the spectral absorption coefficients become slowly varying functions with wavenumber (Penner 1959). Indeed, as noted by Varanasi (1992), with the exception of the central Q-branches, the absorption coefficients for the CFCs remain essentially constant over spectral intervals of order 0.1 cm^{-1}. Moreover, Varanasi (1992) reports that when spectral resolutions between 0.4 and 1.0 cm^{-1} are employed outside of the central Q-branches hardly any discernible differences are observed for the spectral transmittances. As Kratz and Varanasi (1992) noted, the error introduced by employing a resolution of $\sim$0.5 cm^{-1} near the center of the Q-branches can be significant. Nevertheless, they also noted that since the distortion is limited to a very narrow wavenumber range, this effect goes all but unnoticed in applications of the data to climate models. Thus, as Kratz and Varanasi (1992) concluded, a wavenumber resolution of 0.5 cm^{-1} is appropriate for atmospheric modeling.

Since the CFC absorption coefficients are in the smeared-out line structure limit, the use of a line-by-line procedure is not warranted. Instead, it is more appropriate to employ the measured absorption coefficients to determine the spectral absorptance coefficients over each wavenumber interval. For further details of the monochromatic CFC calculations the reader is directed to Kratz and Varanasi (1992).

The reference absorptance calculations were computed for 24 abundances each of CFC-11, CFC-12, and CFC-22 (ranging from 10^{-8} to 3×10^{-4} gm cm^{-2}), and three temperatures (210, 250, and 290 K). For the earth's atmosphere a constant CFC mixing ratio of 1 ppbv corresponds to a CFC-11 abundance of 4.9×10^{-6} gm cm^{-2}, a CFC-12 abundance of 4.3×10^{-6} gm cm^{-2}, and a CFC-22 abundance of 3.1×10^{-6} gm cm^{-2}. Since the CFC absorptances are in the smeared-out line structure limit for atmospheric conditions, the pressure dependence of the CFC absorption coefficients are negligible. As before, an eight-point Gaussian quadrature was incorporated into the monochromatic procedure to calculate the diffuse absorptances.

As noted earlier, parameterizations employing Eq. (1) or similar expressions are utilized by the MLEBM developed at Goddard (Peng et al. 1987) for a variety of infrared absorption bands. It is therefore reasonable to begin with such an equation when attempting to parameterize the absorptances due to the CFCs. Nevertheless, we found that parameterizations employing Eq. (1) met with limited success. The reason is rather straightforward. Gases such as H_2O, CO_2, and O_3 possess a curve of growth that for typical atmospheric conditions spans the range from the weak line region (linear limit) through the strong nonoverlapping line region (square root limit), to the strong overlapping line region. As has been noted previously, Eq. (1) satisfies the requirements for the first two regions, and in a manner similar to the random-band models relies on the exponentiation of the optical depth to handle the last region [see chapter 4 of Goody and Yung (1989) for a discussion of the properties of band models]. Thus, Eq. (1) can adequately describe such a curve of growth. The curve of growth for the CFCs, however, has no strong nonoverlapping line region, for long before the absorption lines begin to saturate they are overlapping their neighbors. Hence, the use of Eq. (1) is inappropriate when considering the CFCs.

As an alternative, let us consider for the moment that Eq. (1) is an approximation that contains only the first term in a series; then we can utilize the other terms in the series to construct a better fit to the reference calculations. A viable series that has several beneficial attributes is given by the expansion of the logarithmic function:

$$\ln(1 + x) = x - \frac{x^2}{2} + \frac{x^3}{3} - \frac{x^4}{4} + - \cdots, \quad (10)$$

where for the present case $x = w(1 + bw^c)^{-1}$. An examination of Eq. (10) reveals that Eq. (1) employs only the first term in this series. If the entire series is utilized, however, then we have an alternative parameterization that is somewhat reminiscent of Eq. (8) from Ramanathan (1976):

$$\tau = a \ln\left(1 + \frac{w}{(1 + bw^c)}\right). \quad (11)$$

This parameterization is easy to implement, efficient, related to Eq. (1) rather than being of a completely different nature, and allows for a direct transition from the weak-line region to a strong overlapping line region. Furthermore, unlike Eq. (1), this expression adequately describes the curve of growth of the absorptances due to the CFCs without introducing unwarranted complexity. Indeed, our investigation has found that parameterizations utilizing Eq. (11) can yield absorptances within 1% of the results of the monochromatic calculations for CFC-11, CFC-12, and CFC-22 for the entire range of temperatures and CFC abundances taken into consideration.

The regression coefficients in our parameterization for the infrared absorption bands of CFC-11, CFC-12, and CFC-22 are presented in Table 4. The temperature dependencies of the regression coefficients are given by:

$$a(t) = a(290) + a'(t - 290), \quad (12)$$

$$b(t) = b(290) + b'(t - 290), \quad (13)$$

where t is the temperature in kelvin. When compared to the 9.4- and 10.4-μm bands of CO_2, the temperature sensitivity of the CFC bands is quite mild; hence, the equations for the temperature dependence of the CFC regression coefficients are far less complex than the temperature dependence of the CO_2 regression coefficients. As with the minor bands of CO_2, the reference temperature was chosen to be 290 K since the contribution of these absorption bands to the opacity of the atmosphere is primarily located within the first few kilometers.

TABLE 4. Parameters for computing CFC-11, CFC-12, and CFC-22 band absorptances. The units for the corresponding abundances, ω, are gm cm^{-2}.

Band	a (290)	a'	b (290)	b'	c
CFC-11 (9.2 μm)	2321.0	2.5875	638.0	−3.900	0.82
CFC-11 (11.8 μm)	11 768.0	13.4750	2085.0	−6.300	0.82
CFC-12 (8.6/9.1 μm)	4397.0	2.300	691.0	−1.625	0.79
CFC-12 (10.8 μm)	4788.0	1.8875	890.0	−2.050	0.79
CFC-22 (9.0 μm)	7601.3	1.1240	1109.7	−0.859	0.78
CFC-22 (12.4 μm)	2737.0	2.7730	386.2	−0.471	0.78

As with the CO_2 calculations of the previous section, the parameterization presented in Eq. (11) requires an inhomogeneous path to be scaled to an equivalent homogeneous path. In contrast to our experience with the minor CO_2 bands, however, our investigation has found that for the CFCs the use of the temperature scaling in Eq. (8) produces accurate results. Note that for the CFCs, the pressure scaling in Eq. (7) is not employed since the CFC absorptances are in the smeared-out limit for typical atmospheric conditions and therefore the dependence of the pressure on the CFC absorption coefficients is negligible.

In order to facilitate a comparison of the present broadband parameterizations to the reference monochromatic calculations we have calculated the reductions in the net upward flux at the top of the atmosphere (50 km) and the tropopause (13 km), and the enhancement in the net downward flux at the surface due to the CFC-11, CFC-12, and CFC-22 absorption bands. As before, to be compatible with the ICRCCM (Ellingson et al. 1991), we employed the midlatitude summer atmosphere of McClatchey et al. (1972), as presented in Ellingson et al. (1991). Based upon measured vertical profiles of the CFCs (see, e.g., Fabian 1987), we have taken the atmospheric mixing ratios of CFC-11 and CFC-12 to be constant from the surface to 15 km. Above 15 km, we have assigned scale heights of 3 and 5 km to the CFC-11 and CFC-12 mixing ratios, respectively. For CFC-22, we have taken the atmospheric mixing ratio to be constant from the surface to 8 km. Above 8 km, we have assigned a scale height of 18 km to the CFC-22 mixing ratio. For each of the CFCs, we have taken the mixing ratio at the surface to be 1 ppbv. The results of our calculations for the 9.2- and 11.8-μm bands of CFC-11, for the 8.6-/9.1- and 10.8-μm bands of CFC-12, and for the 9.0- and 12.4-μm bands of CFC-22 are presented in Table 5. Note that the CFCs are the only absorbers considered for these calculations. Two sets of comparisons are shown in Table 5. In the first set the CFC absorption coefficients are assumed to be the same in the atmosphere as those measured at room temperature (300 K), while in the second set the CFC absorption coefficients are assumed to follow the temperature dependence that was observed in the laboratory (e.g., see Varanasi 1992). As can be observed from Table 5, our parameterizations for the CFCs can reproduce the results of the monochromatic calculations to a very high degree of accuracy. As can also be seen, the temperature dependence leads to only a small modification (~0%–8%) in the flux calculations. Since the temperature de-

TABLE 5. Model calculations of the reduction in the net upward flux (W m^{-2}) at the top of the atmosphere and at the tropopause, and the increase in the downward flux at the surface due to the presence of CFC-11, CFC-12, and CFC-22 with mixing ratios at the surface of 1 ppbv, and above that as noted in the text. Overlapping with water vapor absorption is not considered.

Band	Case	Top	Tropopause	Surface
CFC-11 (9.2 μm)	1	0.109	0.092	0.143
	2	0.105	0.089	0.138
	3	0.100	0.085	0.136
	4	0.100	0.085	0.135
CFC-11 (11.8 μm)	1	0.347	0.300	0.568
	2	0.342	0.295	0.562
	3	0.318	0.277	0.542
	4	0.323	0.281	0.547
CFC-12 (8.6/9.1 μm)	1	0.287	0.237	0.353
	2	0.282	0.232	0.344
	3	0.278	0.230	0.348
	4	0.275	0.227	0.340
CFC-12 (10.8 μm)	1	0.294	0.246	0.441
	2	0.291	0.243	0.432
	3	0.287	0.241	0.435
	4	0.285	0.239	0.428
CFC-22 (9.0 μm)	1	0.236	0.196	0.306
	2	0.236	0.196	0.307
	3	0.234	0.194	0.304
	4	0.234	0.195	0.306
CFC-22 (12.4 μm)	1	0.106	0.090	0.187
	2	0.105	0.089	0.186
	3	0.099	0.085	0.181
	4	0.100	0.086	0.182

Case 1 = monochromatic case (no temperature dependence)
Case 2 = present parameterization (no temperature dependence)
Case 3 = monochromatic case (with temperature dependent absorption coefficients)
Case 4 = present parameterization (with scaled temperature dependence)

pendence of the CFC absorptances is so mild, it is not surprising that the scaling approximation presented in Eq. (8) does not produce significant errors. Recall that this result is quite different from results of the CO_2 calculations.

In contrast to the model presented here, Wang et al. (1991b) adopted the mean absorption coefficient approximation, which can be obtained from our model by taking only the first term in Eq. (10) and assuming that $bw^c \ll 1$, thus

$$\tau(w) = a \ln(1 + w) \approx aw, \qquad (14)$$

for small w. Utilizing Eq. (14) to recompute the flux reductions presented in Table 5 leads an overestimation of 2%–5%. This close agreement indicates that the full power of our parameterization need not be applied for current abundances of the CFCs; however, as noted by Kratz and Varanasi (1992) extrapolation of these results for CFC abundances above 1 ppbv can lead to nonnegligible errors.

In order to compare the results obtained from the present parameterization to those reported by Wang et al. (1991b), we made the following simplifications to our procedure. First, we adopted the mean absorption coefficient approximation given by Eq. (14). Second, we assumed that the CFC absorption coefficients at a temperature of 300 K were appropriate for all temperatures. Third, we assumed that the CFC mixing ratio remained constant throughout the atmosphere. A comparison of the model results for the change in the surface flux are presented in Table 6 for three cases: 1) our present parameterization, 2) our present parameterization with the simplifications described in this paragraph, and 3) the Wang et al. (1991b) model. Note that only surface fluxes are reported in Table 6 since Wang et al. (1991b) did not present results at the top of the atmosphere and presented only partial results at the tropopause. An examination of Table 6 reveals that, when the appropriate simplifications are made to our parameterization, there is good agreement between our results and those of Wang et al. (1991b). Note, however, that the incorporation of these simplifications leads to noticeable overestimations in the radiative impacts of CFC-11 and CFC-12, especially for mixing ratios greater than 1 ppbv. Thus, despite the observation that each of the incorporated simplifications leads to only a small error, when combined the resulting error may no longer be considered acceptable.

4. Overlap with water vapor line and continuum absorption

The ubiquitous water vapor absorption overlaps the absorption bands of CO_2 and the CFCs. It is therefore necessary to take into account the overlapping effect due to water vapor when assessing the radiative effects of these gases. Chou and Arking (1980) and Chou et al. (1991) have demonstrated that Eq. (1) in conjunction with the one-parameter scaling approximation can be used to efficiently compute water vapor absorption in the troposphere. Following the work of Chou (1984), the water vapor amount for line absorption is scaled according to

$$w = w'(p/p_r)^{0.5} \exp[a(t - t_r)] \qquad (15)$$

TABLE 6. Comparisons of the increase in the net downward flux (W m^{-2}) at the surface due to the presence of CFC-11, and CFC-12 for three cases: 1) the present parameterization (see Table 5), 2) the present parameterization with the simplifications described in section 3, and 3) the model of Wang et al. (1991b). Overlapping with water vapor absorption is not considered.

Molecule	Mixing ratio (surface)	Case 1	Case 2	Case 3
CFC-11	1 ppbv	0.68	0.78	0.80
	2 ppbv	1.29	1.53	1.57
CFC-12	1 ppbv	0.77	0.83	0.85
	2 ppbv	1.49	1.65	1.70

where w and w' are the scaled and unscaled water vapor abundances, respectively, p_r is the reference pressure, t_r is the reference temperature, and a is the empirical coefficient for temperature scaling. The reference pressure and temperature are chosen to be 500 mb and 250 K, respectively. From here, the diffuse band absorptance, $A_{diff} = 1 - \exp(-\tau)$, at p_r and t_r can be computed using a line-by-line procedure, and then fit to the function

$$\tau(w) = \frac{bw}{(1 + cw^{0.5})}. \quad (16)$$

Similarly, by following the work of Chou (1984), the band absorptance for the water vapor continuum absorption can be derived using the absorption curve of Roberts et al. (1976) and then fit by

$$\tau(u) = du^{0.92}, \quad (17)$$

where u is the scaled water vapor amount for continuum absorption given by

$$u = w'p_e \exp(1800/t - 6.08), \quad (18)$$

and p_e is the water vapor partial pressure (in atmospheres). Values of the regression coefficients, a, b, c, and d, are given in Table 7 for the spectral regions involving the various minor trace gas absorption bands. The total optical depth, $\tau(w, u)$, due to both line and continuum absorption can be approximated by

$$\tau(w, u) = \tau(w) + \tau(u). \quad (19)$$

The validity of these parameterizations is investigated by comparing the fluxes from the parameterization with the fluxes from the line-by-line procedure. Table 8 shows the upward fluxes at the top of the atmosphere and at the surface in the minor absorption bands. Calculations are for the modified midlatitude summer atmosphere and include both the water vapor line and continuum absorption. It can be seen from Table 8 that the simple parameterizations can accurately compute the fluxes. The error is only a few percent.

Table 9 gives the reduction of net upward fluxes when the trace gas absorptances are overlapped by the water vapor line and e-type continuum absorptances. The multiplication approximation is used to compute the total transmission function due to all absorbers in the parameterization. For the minor CO_2 bands, the parameterizations yield results within 7% of the line-by-line calculations everywhere. For the CFCs, the pa-

TABLE 7. The parameters for computing water vapor absorption in the spectral regions occupied by the trace gases under consideration. The units for the corresponding water vapor abundances, ω and u, are gm cm^{-2}. The band numbers correspond to the wavenumber ranges defined in Table 1.

Band number	a	b	c	d
1	0.020	0.060	1.65	7.35
2	0.020	0.045	1.30	10.22
3	0.020	0.081	1.73	7.07
4	0.026	0.30	6.57	14.68
5	0.019	0.34	4.86	6.84
6	0.024	0.13	3.35	11.82
7	0.020	0.35	4.30	6.60
8	0.020	0.42	4.70	17.30

TABLE 8. Model calculations for the reduction in the net upward flux (W m^{-2}) at the top of the atmosphere and the increase in the downward flux at the surface due to water vapor absorption (line and e-type continuum). The band numbers correspond to the wavenumber ranges defined in Table 1. Overlapping with trace gas absorption is not considered.

Band number	Case	F (top)	F (sfc)
1	1	1.48	11.12
	2	1.40	10.95
2	1	2.07	17.73
	2	2.03	17.91
3	1	1.05	7.73
	2	1.01	7.59
4	1	1.06	9.32
	2	1.04	9.31
5	1	2.20	13.51
	2	2.10	13.31
6	1	2.02	18.16
	2	2.00	17.87
7	1	1.61	9.45
	2	1.70	9.69
8	1	2.85	23.03
	2	2.84	23.39

Case 1 = line-by-line calculation
Case 2 = present parameterization

TABLE 9. Model calculations for the reduction in the net upward flux (W m^{-2}) at the top of the atmosphere and at the tropopause, and the increase in the downward flux at the surface due to the presence of the minor bands of CO_2, CFC-11, CFC-12, and CFC-22 (with the previously noted mixing ratios). Overlapping with water vapor absorption (line and e-type continuum) is considered.

Band	Case	Top	Tropopause	Surface
CO_2 (9.4 μm)	1	0.304	0.285	0.515
	2	0.318	0.304	0.550
CO_2 (10.4 μm)	1	0.233	0.220	0.418
	2	0.244	0.233	0.432
CFC-11 (9.2 μm)	1	0.088	0.073	0.074
	2	0.091	0.077	0.088
CFC-11 (11.8 μm)	1	0.258	0.223	0.188
	2	0.279	0.242	0.249
CFC-12 (9.1/8.6 μm)	1	0.235	0.192	0.178
	2	0.244	0.201	0.211
CFC-12 (10.8 μm)	1	0.245	0.204	0.196
	2	0.253	0.211	0.228
CFC-22 (9.0 μm)	1	0.197	0.162	0.156
	2	0.207	0.171	0.186
CFC-22 (12.4 μm)	1	0.076	0.064	0.050
	2	0.083	0.071	0.067

Case 1 = line-by-line/monochromatic calculation
Case 2 = Present parameterization

rameterizations yield results within 10% of the monochromatic calculations at the top of the atmosphere and the tropopause. At the surface, however, the accuracy of the parameterization is substantially worse; the parameterizations overestimate the flux by 13%–34%. If the water vapor continuum is neglected, these results are dramatically improved: the parameterizations yield results at the surface within 5% for four of the six CFC bands, and by 12%–13% for the remaining two bands. Neglecting the water vapor continuum even improves the parameterized flux calculations at the top and tropopause.

As shown in Tables 5 and 8, separately, the parameterizations for water vapor and the CFCs both yield very good comparisons to the reference calculations. Thus, the relatively large percentage error in the reduction of the net surface fluxes due to the presence of the CFCs, as shown in Table 9, is caused by the use of multiplication approximation for computing total transmittance. An examination of the downward fluxes at the surface reveals that the fluxes due to water vapor are 50 to 500 times greater than those due to the CFCs. It follows that the surface fluxes due to both water vapor and CFC absorption together must be very close to that due to water vapor absorption alone. Thus, to obtain the effect of the CFCs on the surface flux, we must difference two relatively large numbers to obtain a relatively small number. Thus, a small absolute error in the total transmittance using the multiplication approximation can lead to a large percentage error in the surface flux reduction due to the presence of the CFCs.

Recall that the change in the radiative flux at the tropopause, and not the surface, reflects the radiative forcing of the climate system (see, e.g., Ramanathan et al. 1987). Thus, since both the absolute fluxes and the differential fluxes at the tropopause as calculated by the parameterizations and by the reference calculations are in good agreement, the discussed discrepancies do not adversely affect the results of the MLEBM climate calculations. Nevertheless, it is hoped that future modifications will be introduced into the MLEBM to eradicate this difficulty.

As for the reason why the minor CO_2 bands do not suffer a similar fate as the CFC bands, it should be noted that for the case of the minor CO_2 bands, the downward fluxes at the surface due to water vapor are only about 25 to 30 times that due to the minor CO_2 bands. Moreover, the parameterizations for the minor bands of CO_2 underestimate the flux at the surface by 6%–7%, thereby creating a compensating error. These two effects in concert ameliorate the situation as compared to the case of the CFCs.

5. Model description and results

The effects of the anthropogenic increases of CO_2 and the minor trace gases are studied using the zonally averaged multilayer energy balance model of Peng et al. (1987). This model has a five-layer atmosphere, a single mixed layer in the upper ocean, and a simple two-dimensional advective–diffusive deep ocean that allows for a simulation of the long-term climate response to external forcing. The model further includes the effects of seasonal cycles. The temperature, however, is the only prognostic parameter in the model. Transports of heat and fractional surface coverage of snow and sea ice are parameterized as functions of temperature. The relative humidity and clouds are specified as functions of seasons and latitudes.

The model includes a rather detailed treatment of radiative transfer. When computing the radiative heating/cooling for the five atmospheric layers, each layer is divided into three sublayers for proper flux integrations in the vertical. The thermal infrared fluxes are computed using the parameterizations developed in this study and the algorithm of Chou et al. (1991). The algorithm of Chou et al. includes the absorption due to H_2O, CO_2, O_3, CH_4, and N_2O. Except for cirrus, the clouds are assumed to be black in the thermal infrared region. The cirrus clouds are treated as gray with an emissivity of 0.8. The solar fluxes are computed using the algorithms of Chou (1990, 1992) for the absorption due to H_2O, O_3, CO_2, and O_2. The cloud reflection and absorption are computed using the delta-four-stream discrete-ordinate algorithm of Liou et al. (1988).

In addition to the prominent 15-μm CO_2 band, there are a total of 11 minor bands that are considered in this study of the climate greenhouse effect. Three of these bands are the N_2O and CH_4 infrared absorption bands that are presented in Table 3 of Chou et al. (1991), while the others are presented in our Table 1. The relatively narrow bands considered in the present model are scattered within the spectral region between 560 and 1380 cm^{-1}. Incorporation of these bands usually requires regrouping of spectral bands and new parameterizations for transmission functions. In order to simplify the infrared flux calculations, only the change in fluxes due to these minor gases (or bands) is calculated, so that the flux calculations without these minor gases remain unchanged. According to Chou et al. (1991), changes in the net upward flux $\Delta F\uparrow(p)$ at the pressure level p can be expressed as

$$\Delta F\uparrow(p) = B(t_s)\Delta T(p, p_s) - \int_0^{p_s} B(t')\{\partial[\Delta T(p, p')/\partial p']\}\,dp', \quad (20)$$

where B is the band-integrated Planck flux, the subscript s denotes the surface, and $T(p, p')$ is the diffuse transmittance between p and p'. The change in transmittance is given by

$$\Delta T = T_1(T_2 - 1), \quad (21)$$

where T_1 denotes the transmittance due to water vapor absorption, CO_2 absorption in the 15-μm band, or O_3

absorption in the 9.6-μm band, and T_2 denotes the transmittance in the minor absorption bands.

Latent and sensible heat transports in the atmosphere and at the earth's surface are parameterized as functions of temperature. The effect of large-scale eddies is included in the regions poleward of 20° latitude and is parameterized on the basis of quasigeostrophic theory. The effect of the mean meridional circulation is included in the tropics but is neglected in the extratropical regions. The heat convergence due to small-scale eddies is parameterized as a diffusion process. The release of latent heat is computed from the difference between the total moisture convergence due to all scales of motion and the increase in atmospheric moisture storage (with the relative humidity fixed in the model, the atmospheric moisture storage is a function of temperature).

The deep ocean has a large heat capacity and delays the climate response to external forcing. It is represented in the model by two polar regions of downwelling and a vast region of upwelling between ±60° latitudes. Each of the three regions is divided into ten layers of 400-m thickness. The heat exchange between the deep ocean and the ocean mixed layer in the upwelling region depends significantly on the diffusion process. A constant diffusion coefficient of 0.65 $cm^2 s^{-1}$ is used in the upwelling region.

Clouds are grouped into five types: Ci, As, Cu + St, Ns, and Cb. Seasonal cloud cover and heights for the Northern Hemisphere are taken from London (1957). The cloud cover for the Southern Hemisphere is assumed to be 8% larger than the Northern Hemisphere. The cloud cover is also assumed to be composed of randomly overlapped clouds at different altitudes. In addition, our radiative transfer procedure takes the cloud cover as viewed from space to be representative of the cloud cover at all altitudes. Cloud optical thicknesses are extracted from the aircraft measurements of Feigelson (1978) and are specified in the model; these values are given in Peng et al. (1982).

To gauge the potential radiative impact of the minor CO_2 and CFC absorption bands, we have run the MLEBM in its equilibrium mode. The results of these equilibrium cases are presented in Table 10. These results reaffirm the conclusions of previous studies (e.g., Ramanathan et al. 1985) that the potential radiative effects of increases in the CFC abundances are non-negligible in comparison to the radiative effects of increases in the CO_2 abundance. In addition, the results presented in Table 10 clearly support the conclusions of Wang et al. (1991a) that the radiative-forcing behaviors of the trace gases are different from those of CO_2, and thus, as can be deduced from the last column in Table 10, climatic responses can be significantly different for similar radiative forcings at the tropopause. The explanation is that while the radiative forcings at the tropopause may be similar, the vertical distribution of the radiative heating is not. Thus, as noted by Wang et al. (1991b), climate feedbacks in the models may be substantially different.

The radiative forcings presented in Table 10 were also compared to the radiative forcings given by the expressions in Table 2.2 of the IPCC manual (1990). The results of these two quite dissimilar flux calculations were in excellent agreement. Our model was within 1% for CO_2, N_2O, CFC-11, and CFC-12, and about 10% greater for CH_4.

To gain a better understanding of the potential radiative impact of the trace gases, the transient response of the climate to projected trace gas increases has been simulated by the MLEBM for the period from 1900 to 2060. Past trace gas atmospheric abundances were interpolated from Table 2.5 of the IPCC manual (1990), while future trace gas abundances were taken to follow the IPCC low emissions "B" scenario. This functional dependence of the trace gas concentrations with time is presented in Fig. 1. It should be noted that the selection of scenario "B" for future trace gas increases was made in light of the fact that efforts to curb the world production of the radiatively active trace gases make the IPCC business-as-usual "A" scenario unlikely. These same efforts, however, will have to contend with economic pressures that will make the more optimistic IPCC scenarios equally unlikely. It is important to note that the CFC-22 abundance employed by this scenario is meant to represent the abundance of the entire contingent of CFC substitutes. As noted in section 2 of the IPCC manual (1990), the error introduced by employing CFC-22 as a proxy for the CFC substitutes is expected to be small, since most

TABLE 10. Calculations by the MLEBM of the radiative forcings at the tropopause, ΔF_{trop} (W m^{-2}), and the change in the global surface temperature, t_s (K), due to the prescribed changes in the trace gas abundances.

Band	Increase in abundance	Δt_s	ΔF_{trop}	$\Delta t_s/\Delta F_{trop}$
CO_2 (9.4 and 10.4 μm)	345 → 690 ppmv	0.21	0.34	0.62
CFC-11 (9.2 and 11.8 μm)	0 → 1 ppbv	0.17	0.22	0.77
CFC-12 (8.6/9.1 and 10.8 μm)	0 → 1 ppbv	0.21	0.28	0.75
CFC-22 (9.0 and 12.4 μm)	0 → 1 ppbv	0.12	0.17	0.71
CH_4 (7.7 μm)	1.75 → 3.50 ppmv	0.37	0.61	0.61
N_2O (7.8/8.6 and 17 μm)	0.28 → 0.56 ppmv	0.59	0.89	0.66
CO_2 (15 μm)	345 → 690 ppmv	2.40	4.00	0.60

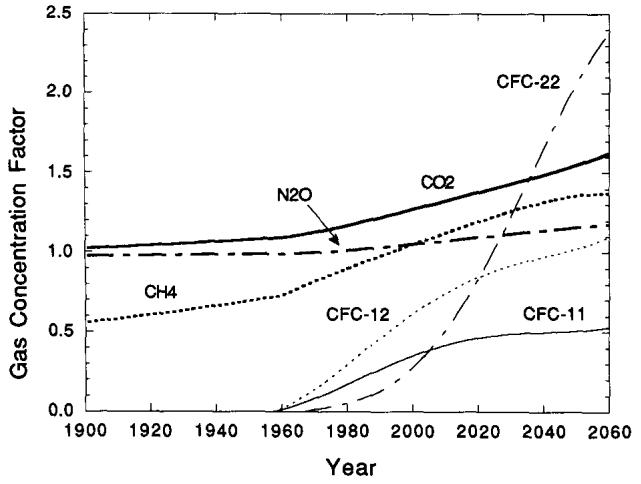

FIG. 1. Temporal dependence of trace gas concentrations for the years 1900 to 2060. Past trace gas atmospheric abundances were interpolated from Table 2.5 of the IPCC manual (1990), while future trace gas abundances were taken to follow the IPCC low emissions "B" scenario. Gas concentration factors equal to one correspond to: $CO_2 = 290 \times 10^{-6}$; $CH_4 = 1.75 \times 10^{-6}$; $N_2O = 0.3 \times 10^{-6}$; CFC-11, CFC-12, CFC-22 $= 1.0 \times 10^{-9}$.

of the HCFCs and CFCs possess similar global warming potential.

The MLEBM simulations of the transient responses are presented in Fig. 2. From this figure, it can be seen that the minor absorption bands collectively account for 40%–45% of the total surface temperature increases. It may also be observed that the increased abundance of CH_4 produces the largest radiative effect among the minor trace gases, amounting to approximately 30% of the effect associated with the absorption due to the 15-μm band of CO_2. While the climatic effects of the CFCs are negligible before 1960, after that date the CFC impact increases rapidly, exceeding the CH_4 effect

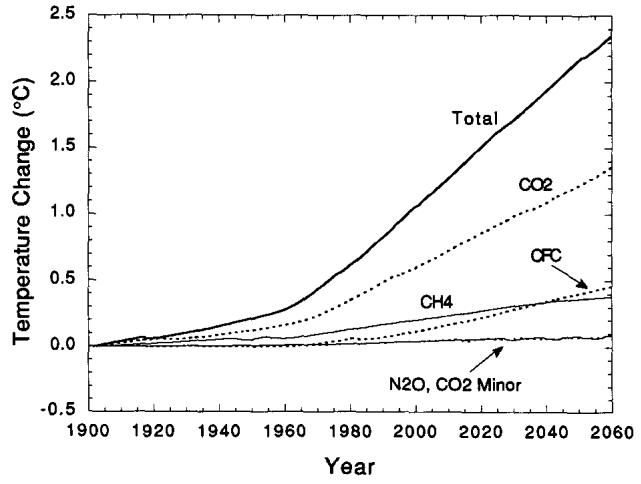

FIG. 2. Transient response of the surface temperature as simulated by the MLEBM for the trace gas increases presented in Fig. 1.

by the middle of the next century. Even without the CFC impact, however, the MLEBM shows an acceleration in the surface temperature increase after 1960. Meanwhile, the climatic effects of the N_2O bands and the two minor CO_2 bands near 10 μm are relatively small and comparable in magnitude. From 1900 to 2060 the model results suggest a surface temperature increase in excess of 2.3 K, with over 1.7 K of that appearing after 1980.

The results of the MLEBM are presented in Table 11 for the period 1960–2030 so as to facilitate a comparison with the results of Hansen et al. (1988). The comparison was terminated at 2030 because the results for the Hansen et al. (1988) scenario B, which has similar trace gas increases as the MLEBM, did not continue beyond that time (see their Fig. 3). The overall surface temperature increase from 1960 to 2030 as calculated by the MLEBM is 1.4 K, virtually the same as illustrated in Fig. 3b of Hansen et al. for their scenario B. It must be noted, however, that the Hansen et al. model has a much greater climatic response to radiative forcings and their associated feedbacks than the MLEBM. This difference should result in a smaller climatic response by the MLEBM when compared to the Hansen et al. (1988) model. It must also be noted, however, that the MLEBM utilizes a significantly smaller ocean diffusion coefficient than the Hansen et al. model, 0.65 $cm^2\ s^{-1}$ versus 1 $cm^2\ s^{-1}$. Since the MLEBM does not transport energy into the ocean as quickly as the Hansen et al. model, the MLEBM will respond faster to a radiative forcing, which compensates for the smaller sensitivity of the MLEBM.

An additional comparison between the models reveals that the Hansen et al. scenario A yields a far greater surface temperature increase for the period 1960–2060: 4.0 K versus 2.3 K from the MLEBM; however, this is primarily due to the slower growth in the trace gas abundance used in the MLEBM.

6. Concluding remarks

During the past decade it has become increasingly obvious that a proper simulation of the potential climatic change caused by anthropogenic activity requires

TABLE 11. MLEBM simulations of the global surface temperature increase, Δt_s (K), from 1960 to 2030 due to IPCC "B" scenario for increases in the trace gases.

Band	Increase in abundance	Δt_s
CO_2 (9.4 and 10.4 μm)	316–415 ppmv	0.055
CFC-11 (9.2 and 11.8 μm)	0.01–0.49 ppbv	0.053
CFC-12 (8.6/9.1 and 10.8 μm)	0.02–0.92 ppbv	0.134
CFC-22 (9.0 and 12.4 μm)	0.00–1.22 ppbv	0.092
CH_4 (7.7 μm)	1.272–2.204 ppmv	0.246
N_2O (7.8/8.6 and 17 μm)	0.297–0.335 ppmv	0.059
CO_2 (15 μm)	316–415 ppmv	0.821

a model to consider the radiative effects of the minor trace gases. To satisfy this requirement, we have developed fast and accurate parameterizations for the absorption due to the CO_2 9.4- and 10.4-μm bands, as well as the CFC-11, CFC-12, and CFC-22 bands located in the 8–12-μm region. These parameterizations are based on line-by-line calculations for the absorption attributed to the CO_2 bands and on high-resolution laboratory measurements of the absorption coefficients for the CFC bands. In order to account for the ubiquitous water vapor absorption that overlaps the absorption bands of CO_2 and the CFCs, we have also developed parameterizations for the absorption features attributed to H_2O for the corresponding spectral bands.

Clear-sky flux calculations that specifically account for the overlap of the absorption features of the trace gases with those of H_2O have demonstrated that the parameterized model is capable of reproducing the results of the high-spectral resolution calculations to within 10% for the flux change at the tropopause. If only the individual trace gas absorptions are considered, the error is much smaller.

The two absorption bands of CO_2 and the six absorption bands of the CFCs encompass eight separate spectral ranges. Incorporation of these bands into the flux algorithm usually requires a repartitioning of the IR spectrum. We have avoided this complication by computing only the flux reductions due to the trace gases under consideration, while leaving the flux calculations without the minor bands unchanged. Hence, incorporation of these trace gas bands into the MLEBM does not disturb the parameterizations of the transmission functions previously incorporated into the MLEBM.

We have studied the climatic effects of these trace gases utilizing a zonally averaged multilayer energy balance model, which includes seasonal cycles and a simplified deep ocean. With the trace gas abundances taken to follow the IPCC low emissions "B" scenario, the transient response of the surface temperature is simulated for the period 1900–2060. The minor absorption bands, including the CH_4 and N_2O bands, collectively account for 40%–45% of the total surface temperature increases. Thus, the climate warming due to absorption in these bands is comparable to that in the 15-μm CO_2 band. Among the minor trace gases, it is found that the increased abundance of CH_4 produces the largest radiative effect. The CH_4 effect is approximately 30% of the effect associated with the absorption due to the 15-μm band of CO_2. Our model results also indicate that the climatic effect of the CFCs increases rapidly with time, exceeding the CH_4 effect by the middle of the next century. The climatic effects of the N_2O bands and the two minor CO_2 bands near 10 μm, on the other hand, are relatively small. Taken as a whole, the MLEBM indicates that for the estimated enhancements of these trace gases the average surface temperature over the period from 1900 to 2060 will realize an increase in excess of 2.3 K, with over 1.7 K of that appearing after 1980.

Acknowledgments. The authors would like to express their deep appreciation to Prof. P. Varanasi for supplying the spectroscopic data for the CFCs that were used in this study. The authors would also like to acknowledge the beneficial comments of the reviewers. The work conducted at Goddard Space Flight Center was supported by the NASA Radiation Processes Program and the NASA Interdisciplinary Research Program.

REFERENCES

Chou, M.-D., 1984: Broadband water vapor transmission functions for atmospheric IR flux computations. *J. Atmos. Sci.*, **41**, 1775–1778.

——, 1990: Parameterizations for the absorption of solar radiation by O_2 and CO_2 with application to climate studies. *J. Climate*, **3**, 209–217.

——, 1992: A solar radiation model for use in climate studies. *J. Atmos. Sci.*, **49**, 762–772.

——, and A. Arking, 1980: Computations of infrared cooling rates in the water vapor bands. *J. Atmos. Sci.*, **37**, 855–867.

——, and L. Peng, 1983: A parameterization of the absorption in the 15 μm CO_2 spectral region with application to climate sensitivity studies. *J. Atmos. Sci.*, **40**, 2183–2192.

——, and L. Kouvaris, 1991: Calculations of transmission functions in the infrared CO_2 and O_3 bands. *J. Geophys. Res.*, **96**, 9003–9012.

——, D. P. Kratz, and W. Ridgway, 1991: Infrared radiation parameterizations in numerical climate models. *J. Climate*, **4**, 424–437.

Dickinson, R. E., and R. J. Cicerone, 1986: Future global warming from atmospheric trace gases. *Nature*, **319**, 109–115.

Ellingson, R. G., J. Ellis, and S. Fels, 1991: The intercomparison of radiation codes used in climate models: Long wave results. *J. Geophys. Res.*, **96**, 8929–8953.

Fabian, P., 1987: Proposed reference models for CO_2 and halogenated hydrocarbons. *Adv. Space Res.*, **7**, (9)63–(9)72.

Feigelson, E. M., 1978: Preliminary radiation model of a cloudy atmosphere. Part I—Structure of clouds and solar radiation. *Beitr. Phys. Atmos.*, **51**, 203–229.

Goody, R. M., and Y. L. Yung, 1989: *Atmospheric Radiation, Theoretical Basis.* Oxford University Press, 519 pp.

Hansen, J., A. Lacis, and M. Prather, 1989: Greenhouse effect of chlorofluorocarbons and other trace gases. *J. Geophys. Res.*, **94**, 16 417–16 421.

——, I. Fung, A. Lacis, D. Rind, S. Lebedeff, R. Ruedy, and G. Russell, 1988: Global climate changes as forecast by Goddard Institute for Space Studies three-dimensional model. *J. Geophys. Res.*, **93**, 9341–9364.

Howard, J. N., D. E. Burch, and D. Williams, 1956: Infrared transmission of synthetic atmospheres IV. Application of theoretical band models. *J. Opt. Soc. Am.*, **46**, 334–338.

Intergovernmental Panel on Climate Change, 1990: Climate Change, the IPCC scientific assessment. Cambridge University Press, 364 pp.

Kiehl, J. T., and V. Ramanathan, 1983: CO_2 radiative parameterizations used in climate models: Comparisons with narrow band models and with laboratory data. *J. Geophys. Res.*, **88**, 7537–7545.

——, and R. E. Dickinson, 1987: A study of the radiative effects of enhanced atmospheric CO_2 and CH_4 on early earth surface temperatures. *J. Geophys. Res.*, **92**, 2991–2998.

Kratz, D. P., and P. Varanasi, 1992: A reexamination of the greenhouse effect due to CFC-11 and CFC-12. *JQSRT*, **48**, 245–254.

——, B.-C. Gao, and J. T. Kiehl, 1991: A study of the radiative

effects of the 9.4 and 10.4 micron bands of carbon dioxide. *J. Geophys. Res.*, **96,** 9021–9026.

Lacis, A., J. Hansen, P. Lee, T. Mitchell, and S. Lebedeff, 1981: Greenhouse effect of trace gases, 1970–1980, *Geophys. Res. Let.*, **8,** 1035–1038.

Liou, K.-N., Q. Fu, and T. P. Ackerman, 1988: A simple formulation of the delta-four-stream approximation for radiative transfer parameterizations. *J. Atmos. Sci.*, **45,** 1940–1947.

London, J., 1957: A study of the atmospheric heat balance, final report. AFC-TR-57-287, OTSPB129551, Coll. of Eng., New York Univ., 99 pp.

McClatchey, R. A., R. W. Fenn, J. E. Selby, F. E. Volz, and J. S. Garing, 1972: Optical Properties of the Atmosphere, third edition. AFCRL-72-0497, Environmental Research Papers No. 411, 108 pp.

Owen, T., R. D. Cess, and V. Ramanathan, 1979: Early earth: An enhanced carbon dioxide greenhouse to compensate for reduced solar luminosity. *Nature,* **277,** 640–642.

Peng, L., M.-D. Chou, and A. Arking, 1982: Climate studies with a multilayer energy balance model. I: Model description and sensitivity to the solar constant. *J. Atmos. Sci.*, **39,** 2639–2656.

——, ——, ——, 1987: Climate warming due to increasing atmospheric CO_2: Simulations with a multilayer coupled atmosphere-ocean seasonal energy balance model. *J. Geophys. Res.*, **92,** 5505–5521.

Penner, S. S., 1959: *Quantitative Molecular Spectroscopy and Gas Emissivities.* Addison-Wesley, 74 pp.

Ramanathan, V., 1975: Greenhouse effect due to chlorofluorocarbons: Climatic implications. *Science,* **190,** 50–52.

——, 1976: Radiative transfer within the earth's troposphere and stratosphere: A simplified radiative-convective model. *J. Atmos. Sci.*, **33,** 1330–1346.

——, R. J. Cicerone, H. B. Singh, and J. T. Kiehl, 1985: Trace gas trends and their potential role in climate change. *J. Geophys. Res.*, **90,** 5547–5566.

——, L. Callis, R. Cess, J. Hansen, I. Isaksen, W. Kuhn, A. Lacis, F. Luther, J. Mahlman, R. Reck, and M. Schlesinger, 1987: Climate-chemical interactions and effects of changing atmospheric trace gases. *Rev. Geophys.*, **25,** 1441–1482.

Roberts, R. E., J. E. A. Selby, and L. M. Biberman, 1976: Infrared continuum absorption by atmospheric water vapor in the 8–12 μm window. *Appl. Opt.*, **15,** 2085–2090.

Rothman, L. S., et al., 1987: The HITRAN database, 1986 edition. *Appl. Opt.*, **26,** 4058–4097.

Sagan, C., and G. Mullen, 1972: Earth and Mars: Evolution of atmospheres and surface temperatures. *Science,* **177,** 52–56.

Varanasi, P., 1992: Absorption coefficients of CFC-11 and CFC-12 relevant to atmospheric remote sensing and global warming studies. *JQSRT,* **48,** 205–219.

Wang, W.-C., and G. Molnar, 1985: A model study of the greenhouse effects due to increasing atmospheric CH_4, N_2O, CF_2Cl_2, and $CFCl_3$. *J. Geophys. Res.*, **90,** 12 971–12 980.

——, G.-Y. Shi, and J. T. Kiehl, 1991b: Incorporation of the thermal radiative effect of CH_4, N_2O, CF_2Cl_2, and $CFCl_3$ into the National Center for Atmospheric Research Community Climate Model. *J. Geophys. Res.*, **96,** 9097–9103.

——, M. P. Dudek, X.-Z. Liang, and J. T. Kiehl, 1991a: Inadequacy of effective CO_2 as a proxy in simulating the greenhouse effect of other radiatively active gases. *Nature,* **350,** 573–577.

——, Y. L. Yung, A. A. Lacis, T. Mo, and J. E. Hansen, 1976: Greenhouse effects due to man-made perturbations of trace gases. *Science,* **194,** 685–689.

Wu, M.-L. C., 1980: The exchange of infrared radiative energy in the troposphere. *J. Geophys. Res.*, **85,** 4084–4090.